N95- 27652

EFFECTS OF LOW EARTH ORBIT ON THE OPTICAL PERFORMANCE OF MULTILAYER ENHANCED HIGH REFLECTANCE MIRRORS*

Terence Donovan
3481 Murdoch Drive
Palo Alto, CA 94306
Phone: 415/424-8990

Linda Johnson, Karl Klemm, Rick Scheri, and Jean Bennett
Naval Air Warfare Center Weapons Division
China Lake, CA 93555-6001
Phone: 619/939-1422, Fax: 619/939-1409

Jon Erickson and Filippo di Brozolo
Charles Evans and Associates
Redwood City, CA 94063
Phone: 415/369-4567, Fax: 415/369-7921

ABSTRACT

Two mirror designs developed for space applications were flown along with a standard mid-infrared design on the leading and trailing edges of the Long Duration Exposure Facility (LDEF). Preliminary observations of induced changes in optical performance of ZnS-coated mirrors and impact-related microstructural and microchemical effects are described in the proceedings of the First LDEF Post-Retrieval Symposium.[1]

In this paper, effects of the induced environment and meteoroid/debris impacts on mirror performance are described in more detail. Also, an analysis of reflectance spectra using the results of Auger and secondary ion mass spectroscopy (SIMS) profiling measurements are used to identify an optical-degradation mechanism for the ZnS-coated mirrors.

Structural damage associated with a high-velocity impact on a (Si/Al_2O_3)-coated mirror was imaged optically and with scanning electron and atomic force microscopy (SEM and AFM). Scanning Auger and SIMS analysis provided chemical mapping of selected impact sites. The impact data suggest design and fabrication modifications for obtaining improved mechanical performance using a design variation identified in preflight laboratory simulations.[2]

Auger surface profile and SIMS imaging data verified the conclusion[1] that secondary impacts are the source of contamination associated with the dendrites grown on the leading-edge ZnS-coated test samples. It was also found that dendrites can be grown in the laboratory by irradiating contaminated sites on a trailing-edge ZnS-coated sample with a rastered electron beam. These results suggest a mechanism for dendrite growth.

---

* Financial support provided by DARPA, USAF Wright Laboratories, and NASA Langley Research Center.

INTRODUCTION

Multilayer-coated test mirrors and single-layer witness samples were flown on both the leading and trailing edges of LDEF. The samples were provided from a DARPA-sponsored program to develop dielectrically-coated high reflectance mirrors for space applications. Two types of mirrors were flown: (1) an industrial standard mid-IR design; (2) two alternative designs that promised improved stability in laboratory simulations of the space environment.[2] The mirrors were contained in vacuum cassettes and exposed for timed periods which varied from 90 to 270 days from the deployment of LDEF. Witness samples consisting of half-wave layers of materials included in the multilayer stacks were exposed for the flight duration. Sample designs and locations on LDEF along with exposure times and atomic oxygen fluences are listed in Table 1.

Table 1. Flight Samples, Location on LDEF, Exposure Time, and Atomic Oxygen Fluence for Experiment Number M0003-7

Sample ID[a]	Design	LDEF location[b]	Exposure (months)	Atomic Oxygen Fluence (atoms/cm^2)
L6-VI-7-46-11	$(Si/Al_2O_3)^3Ag/Si$	D8	3	$3.1x10^{20}$
T6-VI-7-31-4	$(Si/Al_2O_3)^2Ag/Mo$	D4	3	$9.9x10^{3}$
L3-II-7-61-3	Si/fused silica	D9	70	$9.0x10^{21}$
T3-II-7-60-4	" " "	D3	70	$1.3x10^{17}$
L6-VI-7-68-15	$(ZnS/ThF_4)^5Ag/Mo$[c]	D8	6	$6.1x10^{20}$
T6-VI-7-30-36	" " " "	D4	9	$3.0x10^{4}$
L3-II-7-65-10	ZnS/fused silica	D9	70	$9.0x10^{21}$
T3-II-7-64-11	" " "	D3	70	$1.3x10^{17}$
L6-VI-7-67-239	$(ZnS/Al_2O_3)^4Ag/Mo$	D8	9	$9.2x10^{20}$

[a] Sample ID provides the tray, module, sub-experiment, module location, and sample numbers
[b] Row numbers: leading edge (D8, D9); trailing edge (D3, D4)
[c] Industrial-standard, mid-IR design

The post-flight optical, surface/profiling, and impact-related data on test mirrors and witness samples listed in Table 1 are discussed in this paper along with an analysis of the factors found detrimental to optical performance. These results along with laboratory simulation data are used to suggest an alternative coating design and fabrication process for improved mirror performance.

$(Si/Al_2O_3)^nAg/Si$ MIRROR DESIGN RESULTS

The spectral reflectance of the leading-edge $(Si/Al_2O_3)^3Ag/Si$ test sample after 90 days exposure to the effects of low-Earth orbit (LEO) is shown in Figure 1. As seen in the figure, the reflectance of the test sample is reduced less than 0.1% at the design wavelength (2.8 μm) relative to the laboratory control. The reflectance of the control was reduced by less than 0.1% after 10 years on the laboratory shelf. Profilometer measurements showed that increases in optical scatter resulted from surface debris and not

from changes in microstructure or topography. The scatter increase contributed to the small reflectance loss relative to the control.

Auger profiles of the test sample are shown in Figures 2 and 3. The depth profile (Figure 2) reveals the design; three Si/Al_2O_3 high/low index pairs, a Ag reflectance enhancing layer, and the silicon substrate. Some charging occurred during sputter etching of the third silicon layer but the thicknesses are fairly uniform. Note the small Ag peak at the outer Si/Al_2O_3 interface and a C contamination peak at the Al_2O_3/Ag interface.

An Auger surface profile is shown in Figure 3. The estimated sputter rate and time to when oxygen reaches the background level indicates approximately 36 Å of surface oxide. This is within a factor of two of what one would expect from a natural oxide layer on silicon. It is noted that the small growth rate relates to the atomic oxygen (AO) flux at the deployment altitude (476 km) and the short exposure (3 months). This thickness will have little effect at the design wavelength but could account for a slight increase in absorption at wavelengths greater than 3 μm.

Rutherford backscattering spectrometry (RBS) measurements were made on two single-layer Si witness samples that were exposed for the 70-month flight duration (AO fluence: D9 = $9.0x10^{21}$ atoms/cm^2; D3 = $1.3x10^{17}$ atoms/cm^2). An average of 20 atomic % O was found in the outer 900 Å on the leading-edge witness (L3-II-7-61-3) and relates to the long exposure and significantly higher average AO-flux levels than were experienced by the test mirror (L6-VI-7-46-11). In contrast, no surface oxidation was detected by RBS on the trailing-edge witness (T3-II-7-60-4).

One impact site was observed on the test mirror. The 10-μm-diameter x 0.6-μm-deep impact crater is shown in Figure 4a. The effective damage area was increased by the radial and spiral fractures shown in Figure 4a and delamination in the crater vicinity as shown in a scanning atomic force micrograph (AFM) in Figure 4b. An impacting particle of carbon was identified by scanning Auger microscopy; silver was detected along the spiral fracture. The Auger profile in Figure 2 suggests the Ag migrated from the reflectance-enhancing layer to the surface, thermally driven by the impact. The extended structural damage severely limits the potential performance of the mirror.

A larger, 50-μm-diameter crater was found on the Si/fused silica witness, T3-II-7-60-4. The crater is enriched in K, Cl, O, $(SO_2)^-$, SiO_2, and $(OH)^-$. Au and Au^+ were also seen in the time-of-flight secondary ion mass spectroscopy (SIMS) data. K was concentrated in the crater and probably originated from a less-energetic, secondary impact. In this case, no extended structural damage was observed.

DISCUSSION OF $(Si/Al_2O_3)^nAg/Si$ MIRROR DESIGN RESULTS

The $(Si/Al_2O_3)^3Ag/Si$ design is optically stable in an ionizing-radiation environment as predicted by extensive laboratory simulations[2] and confirmed by the LDEF flight. AO flux at the deployment altitude and for a limited exposure period has little effect on mirror performance at the design wavelength. Impacts, on the other hand, because of associated structural effects (delamination and fracture) can lead to severe mirror degradation and failure.

The design can be improved by the elimination of Ag as a reflectance-enhancing layer and the substitution of SiO_2 for Al_2O_3 as the low-index component. Ag can melt and diffuse at temperatures generated by particle impacts. Si/SiO_x multilayers were shown to be stable in a combined solar-UV/charged-particle environment in preflight laboratory simulations.[2] Si/SiO_2 multilayers can be

deposited directly on silicon using a reactive sputtering process. This will result in lower stress, increased adhesion, and a reduction in the possibility of delamination and fracture induced by high-velocity impacting particles.

$(ZnS/Al_2O_3)^4Ag$ MIRROR DESIGN RESULTS

The post-flight reflectance of the leading-edge $(ZnS/Al_2O_3)^4Ag$ test sample compared to a laboratory control is shown in Figure 5. The mirror was exposed for nine months beginning with the deployment of LDEF. The test sample has an absorption band centered at 3 μm which reduces the reflectance at the design wavelength of 2.8 μm. The control has no similar loss.

Surface profilometry measurements show an increase in roughness (and related scatter) compared with preflight data. The increase is due to some degradation of the coating surface, debris, and the presence of dendritic material. The scatter, degraded material, and areas of dendritic growth, however, do not account for the spectral feature.

A depth profile of this sample taken by SIMS is shown in Figure 6. Sputter etching was accomplished using O^- primary ions to minimize charging effects. The layers are uniform in thickness and there are no significant deviations from the quarter-wave design to account for the spectral band, suggesting the absorption is due to water contamination. Unfortunately, an analysis of H and O couldn't be obtained by sputtering with O^- primary ions.

$(ZnS/ThF_4)^5Ag$ MIRROR DESIGN RESULTS

Similar spectral bands, in this case centered at 2.9 μm, are observed in the post-flight reflectance data of both leading- and trailing-edge ZnS/ThF_4 test samples. SIMS profiling data is shown in Figure 7 for the leading-edge sample. Here, atomic concentration versus depth is plotted with sputter time converted to depth with stylus profilometry using the assumption that ZnS and ThF_4 sputter at equal rates. Sputter etching was accomplished in this case with Cs^+ primary ions, which can be used to determine H and O. Charging is somewhat of a problem with Cs^+, but the data is in qualitative agreement with Auger profile data[1] which also shows a relatively thin surface and thick base layers of ZnS.

SIMS depth profiles of O and H are shown in Figures 8 and 9, respectively, for this sample. Calibration in terms of atomic concentration was done using data from float-zone-refined silicon. Note the presence of H and O in the ThF_4 layers with tendency of both materials to peak at high/low index interfaces. Also, concentrations of O and particularly H tend to increase with depth into the coating. It is possible that water contamination incorporated during fabrication was ionized in the radiation environment of LDEF and moved to the film interfaces driven by a reduction in free-energy.

Thin-film design software[3] and literature values[4,5] for the optical constants of ZnS, ThF_4, and Ag were used to model the observed post-flight reflectance spectra. Two approaches were taken using the SIMS and Auger data.

In the first approach, only the thicknesses of the ZnS and ThF_4 layers were varied in the reflectance calculation. The thickness variations either were derived from experimental data (i.e., the SIMS depth profiles) or were arbitrarily chosen to try to force the calculated curve to fit the observed reflectance

spectra. With this approach it was not possible to reproduce either the spectral position or the magnitude of the absorption band centered at 2.9 μm.

The second approach used both the layer thickness variations and the water contamination observed at the interfaces in the SIMS depth profiles. Optical constants for thin layers of water[6] were entered into the reflectance calculation along with the layer thickness variations derived from the SIMS data. The optimum water contamination (10 Å/interface) was determined by iteration within the range of possible values determined by SIMS.

The calculated spectral reflectance values are compared with post-flight reflectance data in Figure 10. As seen in the figure, the SIMS data gives an excellent fit to the reflectance spectrum in the 2.9 to 4.0 μm region. This result validates preflight simulations of combined solar-UV/charged-particle radiation at the Boeing Radiation Effects Laboratory[2] which showed that the irradiation of water-contaminated ZnS/ThF_4 multilayers increased the optical absorption about 1% at 2.9 μm.

IMPACT DAMAGE, CONTAMINATION, AND EFFECTS OF THE SOLAR UV/ATOMIC OXYGEN ENVIRONMENT

Two types of impact damage found on the ZnS-coated mirrors were described earlier;[1] craters formed by high-velocity impacts and secondary impacts associated with copper contamination. Copper and other contaminants have been found by Auger and SIMS analysis on the leading- and trailing-edge ZnS mirrors. Cu is associated with dendrite growth on leading-edge test samples.[1] A third type of damage with crater-like features was found in the raster-pattern areas that were sputter etched during SIMS depth-profiling measurements.

Figure 11 shows one of two craters formed by high-velocity impact on leading-edge sample L6-VI-7-68-15. This crater is about 70 μm in diameter and about 3.5 μm deep and was formed by a particle approximately 10 μm in diameter. The multilayer structure is exposed, revealing melt and some undercutting of the individual layers suggesting their vulnerability to attack by solar UV/atomic oxygen. An analysis was not performed for possible residual material from the impacting particle.

Figures 12a and 12b show optical and AFM images of one of four sites found on trailing-edge sample T6-VI-7-30-36. The crater is irregular in shape and about 1 μm deep. Melted material estimated by AFM to be 2000 Å thick is spewed in a radial fashion from the impact site. SIMS analysis in the region of two other impact sites (smaller craters) on this sample identified Cu, Al, Na, K, and siloxane contaminants. The Cu probably originated from diamond-turned Cu mirrors in the sample module.

A large number of dendrites were observed by optical microscopy during de-integration of the two leading-edge ZnS test samples.[1] Figures 13a and 13b show optical images of dendrites grown in orbit on samples L6-VI-7-68-15 and L6-VI-7-67-239. These and other dendrites are surface features that appear to result from a thermal (melt/solidification) growth process.[7]

A high-contrast SEM image and scanning Auger analysis of a dendrite described earlier[1] suggest a reaction with Cu to form a CuZn or CuZnS alloy. An Auger depth profile (Figure 14) taken in a region of dendrites gives a direct indication of a displacement reaction between Cu and ZnS. This profile also shows that O has to some extent replaced S in the ZnS. The thickness of the "alloy" and oxide is estimated from the sputter time to be about 400 Å. A mass-resolved SIMS image of a dendrite at an Al-contaminated site on the leading-edge ZnS/ThF_4 test sample is shown in Figure 15.

No dendrites were found on the trailing-edge sample, but they could be grown in the laboratory by rastering an electron beam in the vicinity of an impact site. The electron-stimulated growth of dendrites was recorded on video tape. An SEM image of a dendrite grown by electron irradiation is shown in Figure 16. The spherical particles, shown in the figure, appeared as a result of electron irradiation. The depletion of these "clusters" in the vicinity of the dendrite suggests a diffusion-limited growth process. Nucleation and growth possibly initiated at the small damage site in the upper left branch of the dendrite shown in Figure 16.

ZnS is known to dissociate in a UV environment and react with oxygen[8] to form the oxide. Evidence for the occurrence of this reaction in LEO is provided by RBS analysis and optical micrographs (Figure 17) of leading- and trailing-edge witness samples of ZnS exposed for the 70-month duration of LDEF. The leading-edge sample is 15 atomic % O throughout as estimated by RBS. The coating has buckled and, as seen in Figure 17a, annular features are observed at high magnification. The composition and origin of these features has not been determined. The trailing-edge sample (Figure 17b) is mostly intact but many blisters, perhaps related to locally poor adhesion, are observed at high magnification. This sample is not oxidized.

Finally, several crater-like features were found in the ion-raster patterns during profiling-SIMS measurements of sample L6-VI-7-68-15. A raster pattern with small crater-like features is shown in Figure 18a. A profilometer trace through one of the craters is shown in Figure 18b. The crater is 40 μm in diameter and about 2.4 μm deep. The "craters", which were observed after profiling, developed when a 14.5 kV, 0.1 to 0.7 mA Cs^+ primary ion beam was rastered over a square region 500 μm on a side.

DISCUSSION OF ZnS COATING RESULTS

All ZnS coatings had significant reflectance losses at the design wavelength. The reflectance losses, based on modeling of sample L6-VI-7-68-15, are attributed to deviations from the quarter-wave design thicknesses and absorption increases due to $(OH)^-$ accumulation at interfaces between high and low index coating layers. It is suggested that water present as an impurity in the coatings was ionized in the charged particle (e^- and p^+) environment and the mobile ions moved to film interfaces where a reduction in system free energy can occur. Similar in-band absorption increases were observed in preflight laboratory simulations.[2]

Primary and secondary impact damage, surface contamination, oxidation, and extensive dendrite formation also contributed directly to the optical degradation of these mirrors.

Dendrite formation, which occurred in orbit on samples flown on the leading edge of LDEF, is attributed to displacement reactions of primarily Cu and Al contamination with Zn to form alloys. A phase change from face-centered-cubic to body-centered-cubic Cu is suggested as a possible driving force for the displacement reaction; AO could provide thermal energy for the Cu diffusion and also react with Zn^{++}, created by the UV dissociation of ZnS, to form the oxide.

The Cu and possibly Al contamination originated from secondary impacts from other mirrors in the sample modules. The electron-stimulated growth of dendrites observed in the laboratory on the trailing-edge mirror (T6-VI-7-30-36) suggests a diffusion-rate-limited growth process. Growth was observed, in the laboratory, to initiate (and presumably nucleation occurred) at secondary impact sites.

The crater-like features that developed as the result of Cs^+ ion etching during SIMS profiling may result from displacement damage, possibly of cosmic ray origin. Further study will be required to understand the origin, extent, and effect of these features on mirror performance.

CONCLUSIONS AND SUGGESTIONS FOR FURTHER WORK

The LDEF flight established the validity of laboratory simulations in screening coated optics for applications in the space environment. Preflight laboratory simulations predicted the optical stability of silicon/oxide designs and identified a potential water-impurity problem in the ZnS designs.[2] Impact damage, both primary and secondary, was identified as a serious degradation mechanism for both silicon and zinc sulfide designs.

A reactively sputtered $(Si/SiO_2)^n/Si$ design is suggested as a low-stress, adherent alternative to the optically-stable but impact-damage-susceptible-$(Si/Al_2O_3)^nAg/Si$ and chemically-unstable-ZnS designs flown on LDEF.

The ZnS designs suffered reflectance losses, impact damage, surface contamination, oxidation, and extensive dendrite growth, all of which contributed to degradation of the mirrors. Deviations from quarter-wave thicknesses and water contamination identified in SIMS-depth profiles successfully accounts for reflectance loss in the 3-μm-spectral region. The dendrites are associated with displacement reactions of primarily Cu contamination with ZnS. It is suggested that the energy for the diffusion-limited-growth process was supplied by energetic (5eV) AO impacting the leading-edge test mirrors.

Finally, crater-like features that developed deep in a ZnS/ThF_4 coating during SIMS-profiling analysis should be studied in more detail to determine if they are impact related and of extraterrestrial origin. Ultimately, the effect of these craters on mirror performance should be assessed.

ACKNOWLEDGMENTS

Integration and de-integration was accomplished by the Aerospace Corporation (experiment M0003). The authors also thank T. Beirling and R. Helms of Stanford University for Auger surface profile measurements and R. Feigelson, also of Stanford University, for discussions of dendrite growth.

REFERENCES

1. Donovan, T. M.; Bennett, J. M.; Dalbey, R. Z.; Burge, D. K.; and Gyetvay, S.: Space Environmental Effects on Coated Optics. Presented at the First Post-Retrieval Symposium for LDEF, Kissimmee, Florida, 2-8 June 1991. NASA Conference Publication 3134, Part 3, pp. 1361-76.

2. Fogdall, L. B.; Cannaday, S. S.; Gellert, R. I.; Polky, J. N.; and Davies, F. W.: Natural and Induced Space Radiation Effects on Optical Coatings and Materials. Boeing Radiation Effects Laboratory Final Report submitted to the Naval Weapons Center, China Lake, California on Contracts N00123-78-C-0989 and N60530-79-C-0263, April 1981.

3. Macleod, H. A.: *Macleod Thin-Film Design Software.* Thin Film Center, 2745 East Via Rotonda, Tucson, Arizona.

4. Palik, E. D., ed.: *Handbook of Optical Constants of Solids.* Academic Press, Inc., Orlando, Fla., 1985.

5. Palik, E. D., ed.: *Handbook of Optical Constants of Solids II.* Academic Press, Inc., San Diego, Calif., 1991.

6. Rusk, A. N.; Williams, D.; and Querry, M. R.: Optical Constants of Water in the Infrared. *J. Opt. Soc. Am.*, vol. 61, (1971), pp. 895-903.

7. Langer, J. S.; Issues and Opportunities in Materials Research. *Physics Today*, vol. 45, no. 10, October, 1992.

8. Hass, G.; Heaney, J. B.; Hunter, W. R.; and Angel, D. W.: Effect of UV Radiation on Evaporated ZnS Films. *Appl. Opt.*, vol. 19, (1980), pp. 2480-81.

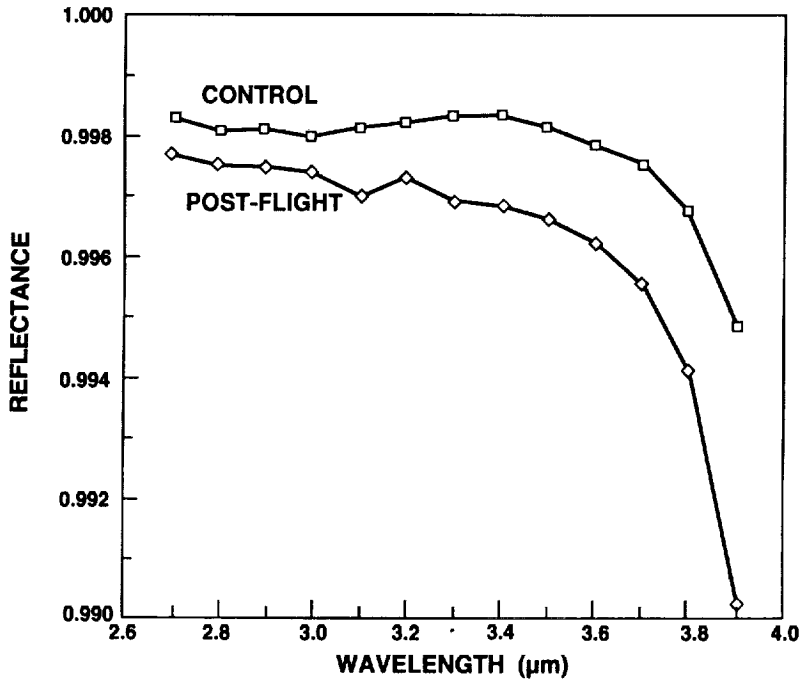

Figure 1. Post-flight reflectance of the leading-edge $(Si/Al_2O_3)^3Ag/Si$ test sample compared to a laboratory control. The reflectance loss of the test sample relative to the control is less than 0.1% at the design wavelength (2.8 μm).

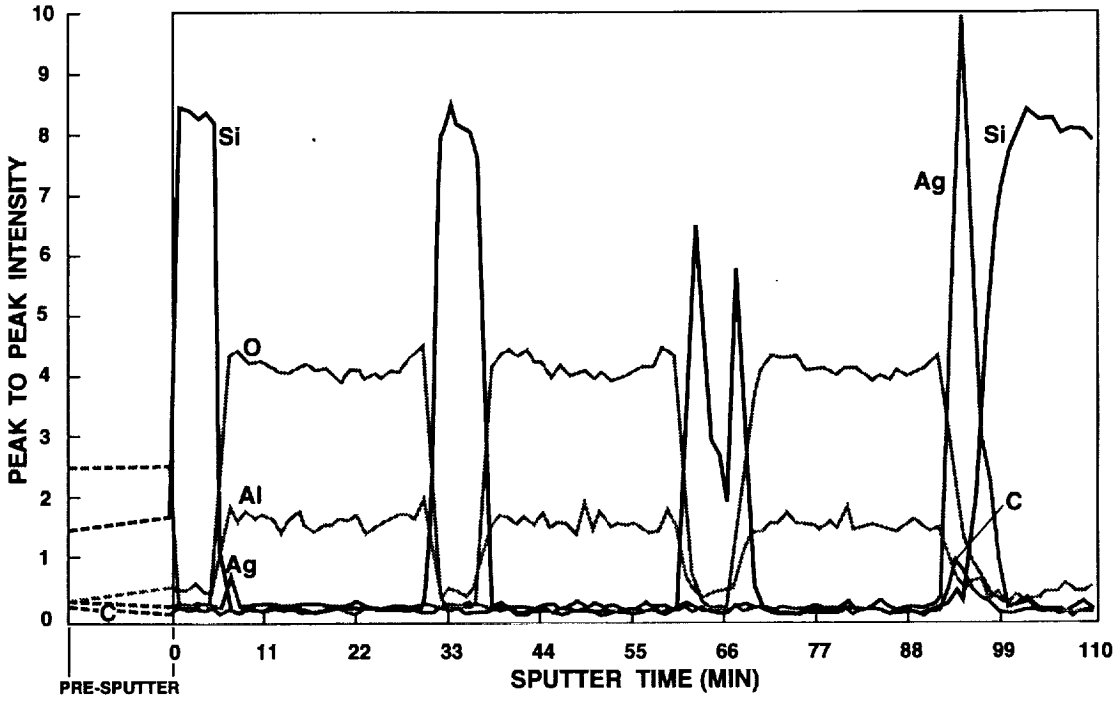

Figure 2. Post-flight Auger depth profile of the leading-edge $(Si/Al_2O_3)^3Ag/Si$ test sample showing uniform layer thicknesses. Distortion of the third Si layer peak is due to surface charging.

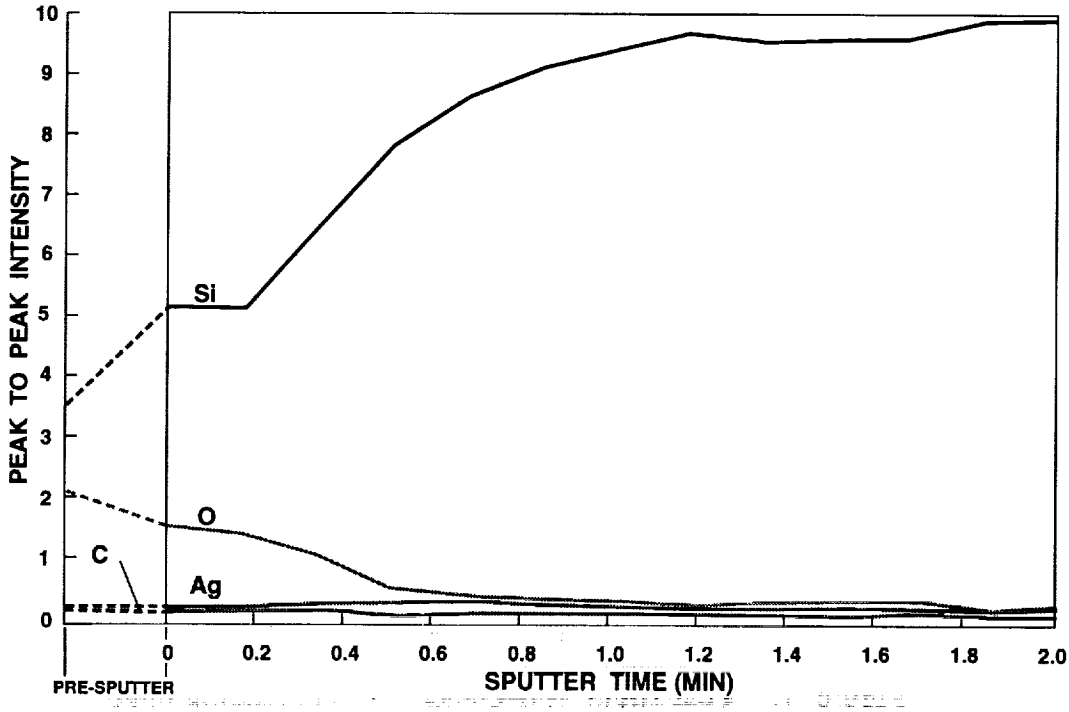

Figure 3. Post-flight Auger surface profile of the leading-edge $(Si/Al_2O_3)^3Ag/Si$ test sample. The thin surface oxide layer indicates that Si is not significantly degraded by the energetic AO encountered in LEO.

10 μm

Figure 4a. Scanning electron micrograph showing radial and spiral fractures extending from the impact crater on the leading-edge $(Si/Al_2O_3)^3Ag/Si$ test sample.

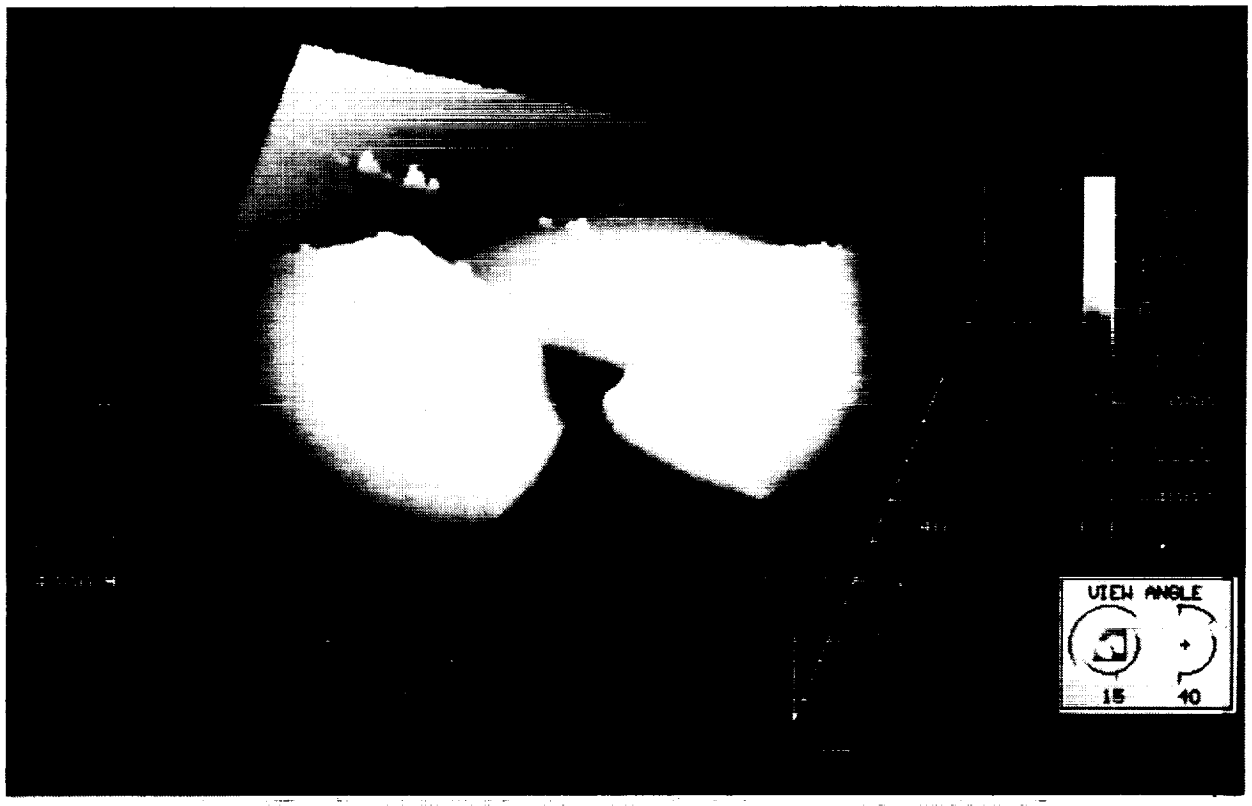

Figure 4b. Atomic force micrograph of impact site in Figure 4a showing the impact crater and film delamination surrounding the crater.

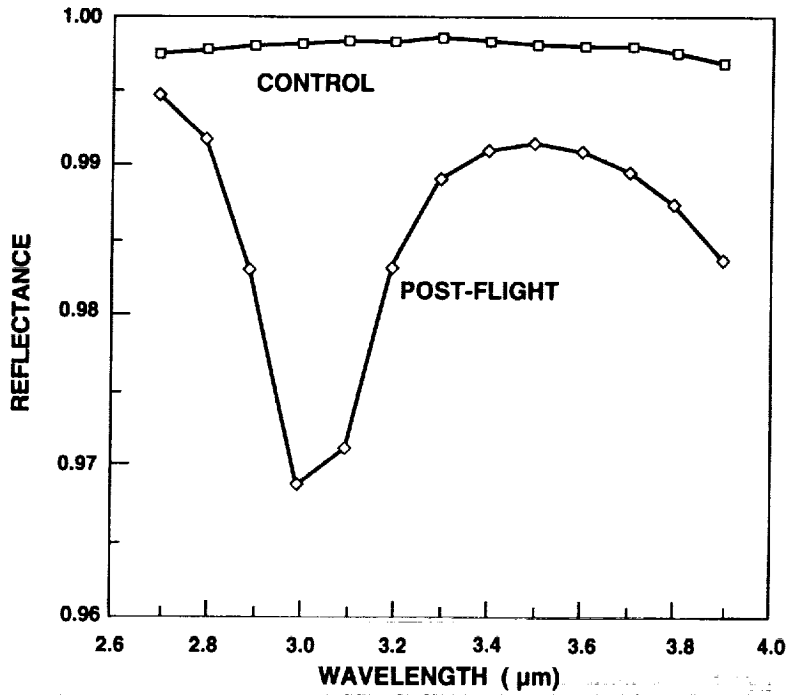

Figure 5. Post-flight reflectance of the leading-edge $(ZnS/Al_2O_3)^4Ag/Mo$ test sample compared to a laboratory control.

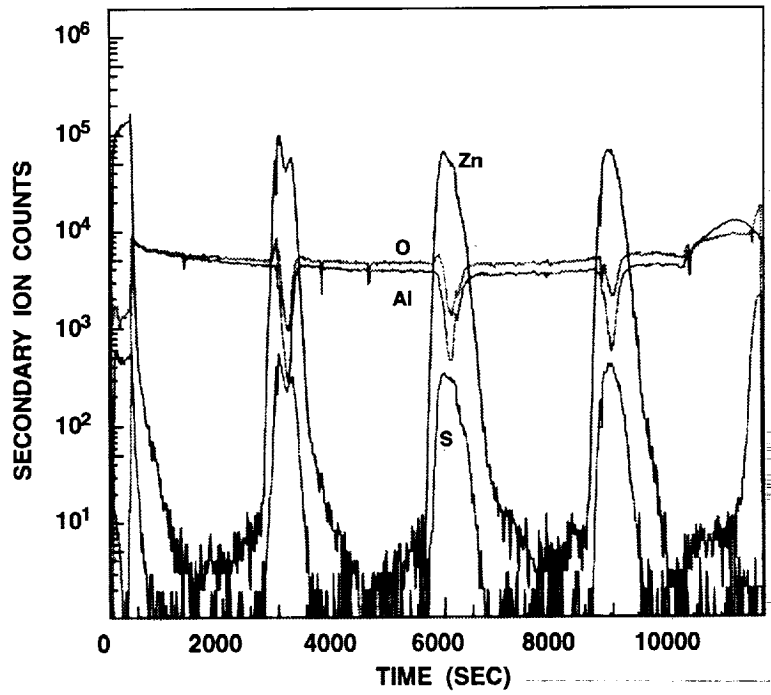

Figure 6. SIMS depth profile of the leading-edge $(ZnS/Al_2O_3)^4Ag/Mo$ test sample showing uniform layer thicknesses.

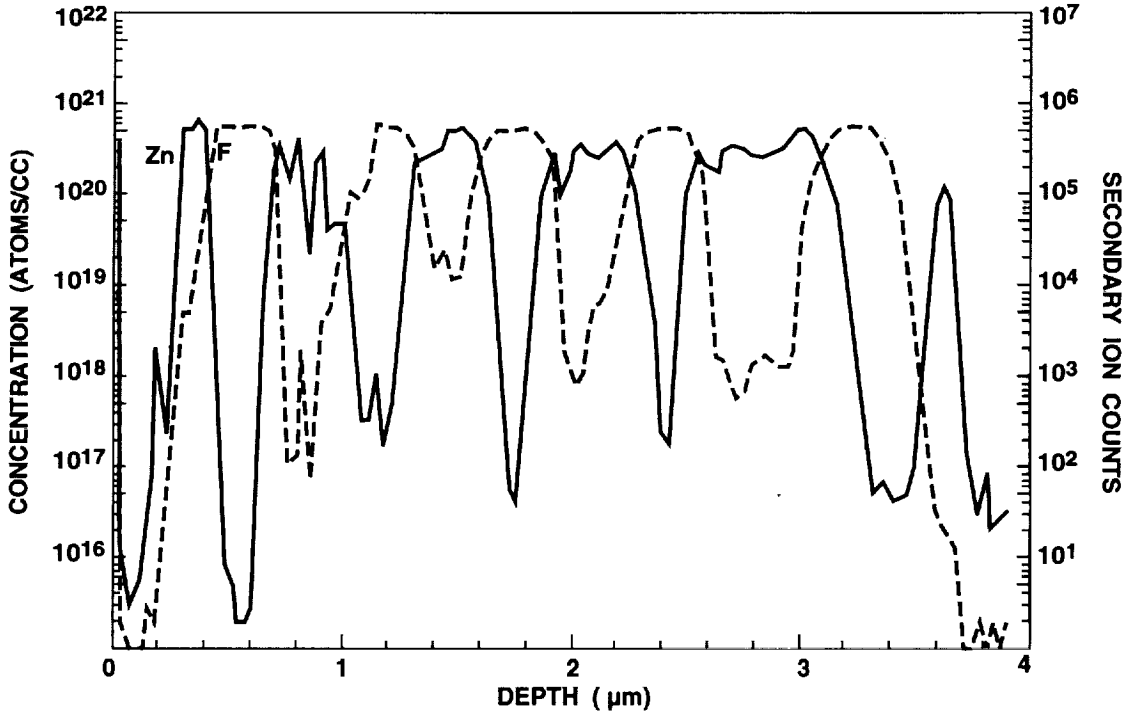

Figure 7. SIMS depth profile of the leading-edge $(ZnS/ThF_4)^5Ag/Mo$ test sample showing a thin surface layer and thick base layers of ZnS.

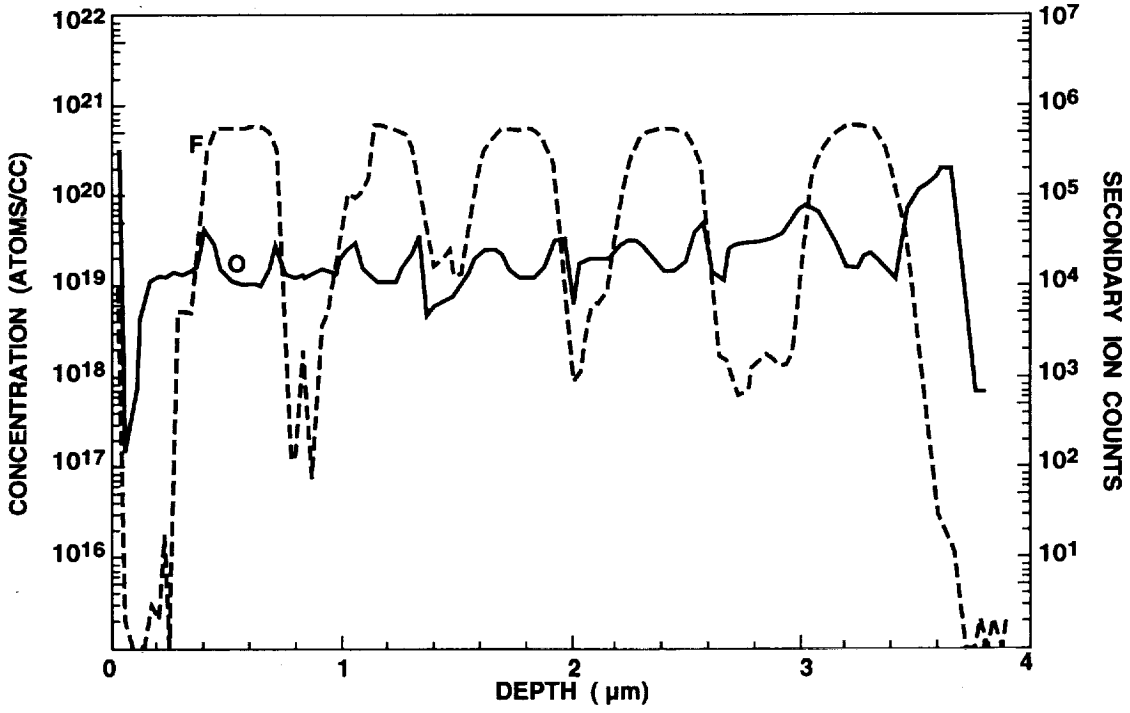

Figure 8. SIMS depth profile of the leading-edge $(ZnS/ThF_4)^5Ag/Mo$ test sample. The O concentration peaks at the interfaces and increases with depth into the coating.

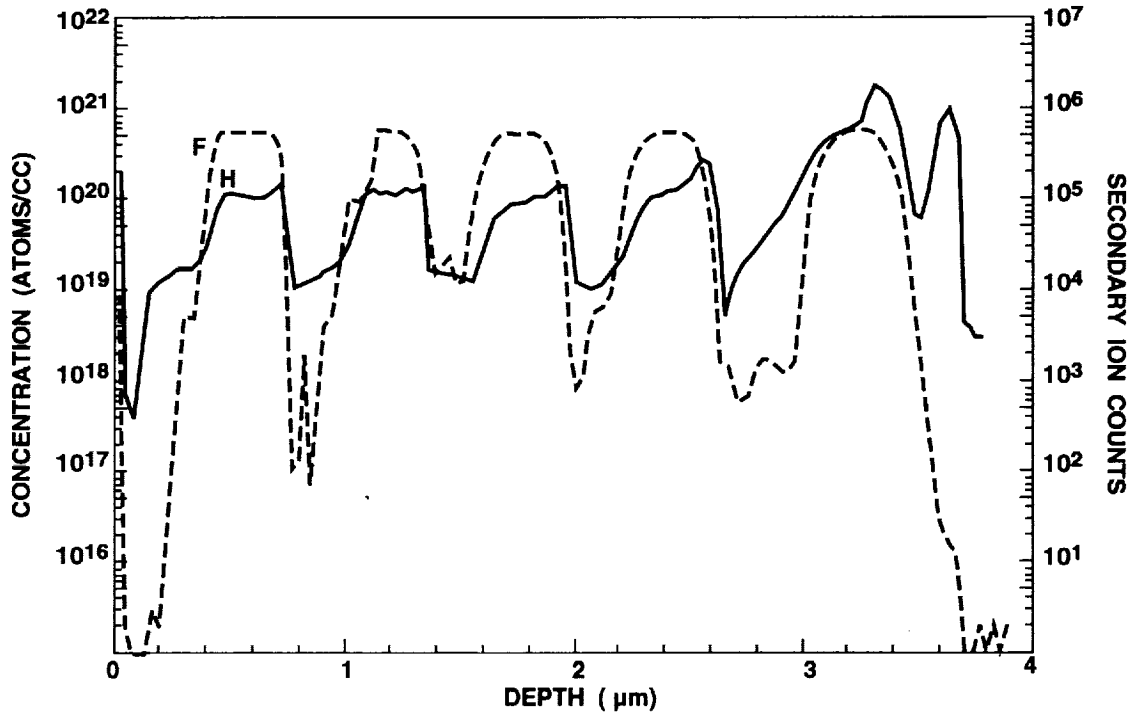

Figure 9. SIMS depth profile of the leading-edge $(ZnS/ThF_4)^5Ag/Mo$ test sample. The H concentration is high in the ThF_4 layers and increases with depth into the coating.

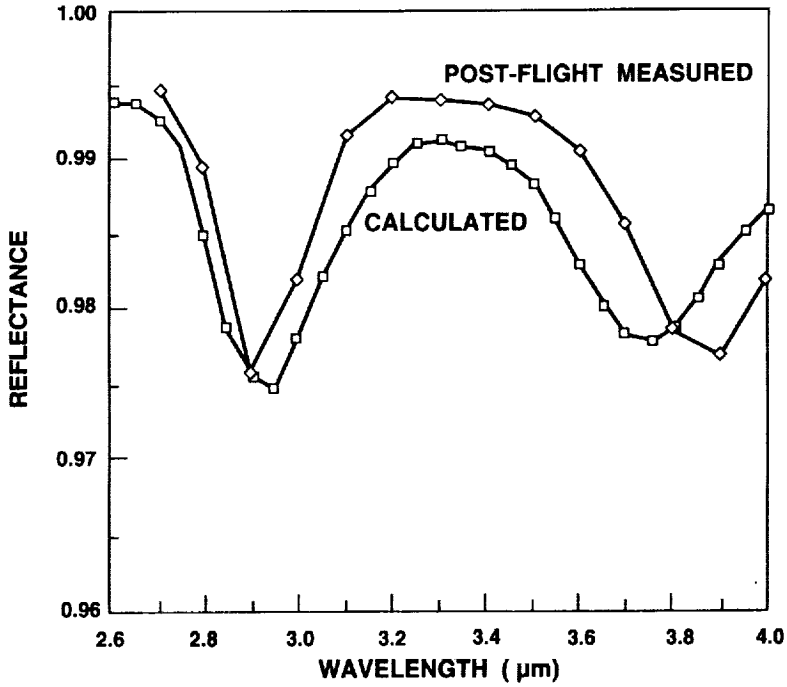

Figure 10. Measured post-flight reflectance of the leading-edge $(ZnS/ThF_4)^5Ag/Mo$ test sample compared to a calculated reflectance curve. Thin layers of water contamination at film interfaces and layer thicknesses derived from the SIMS data shown in Figures 7-9 were used to match the calculated to the measured reflectance curve.

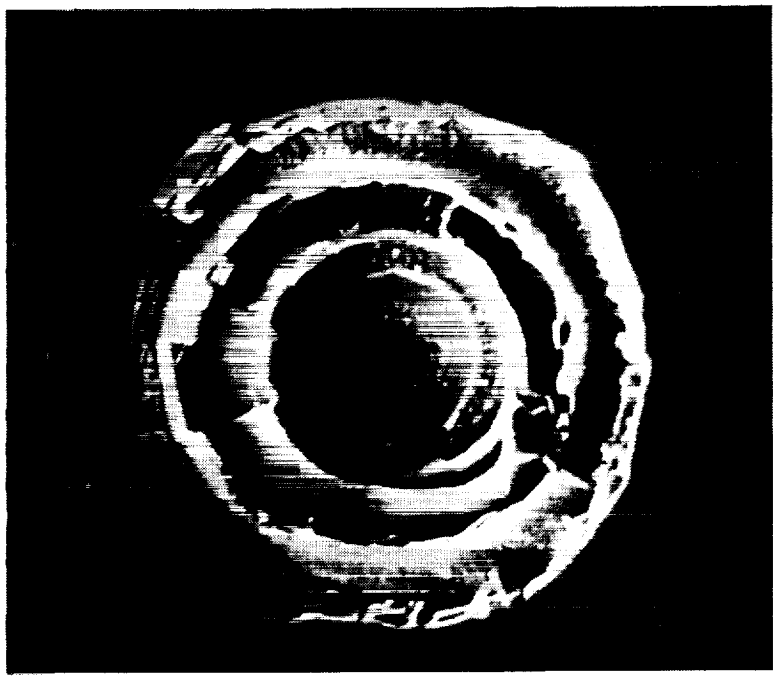

10 μm

Figure 11. Scanning electron micrograph of impact crater on leading-edge $(ZnS/ThF_4)^5Ag/Mo$ test sample revealing the multilayer structure and melt of individual layers.

Figure 12a. Optical micrograph of secondary impact crater on trailing-edge $(ZnS/ThF_4)^5Ag/Mo$ test sample. (Micrograph courtesy of S. Gyetvay, Aerospace Corporation.)

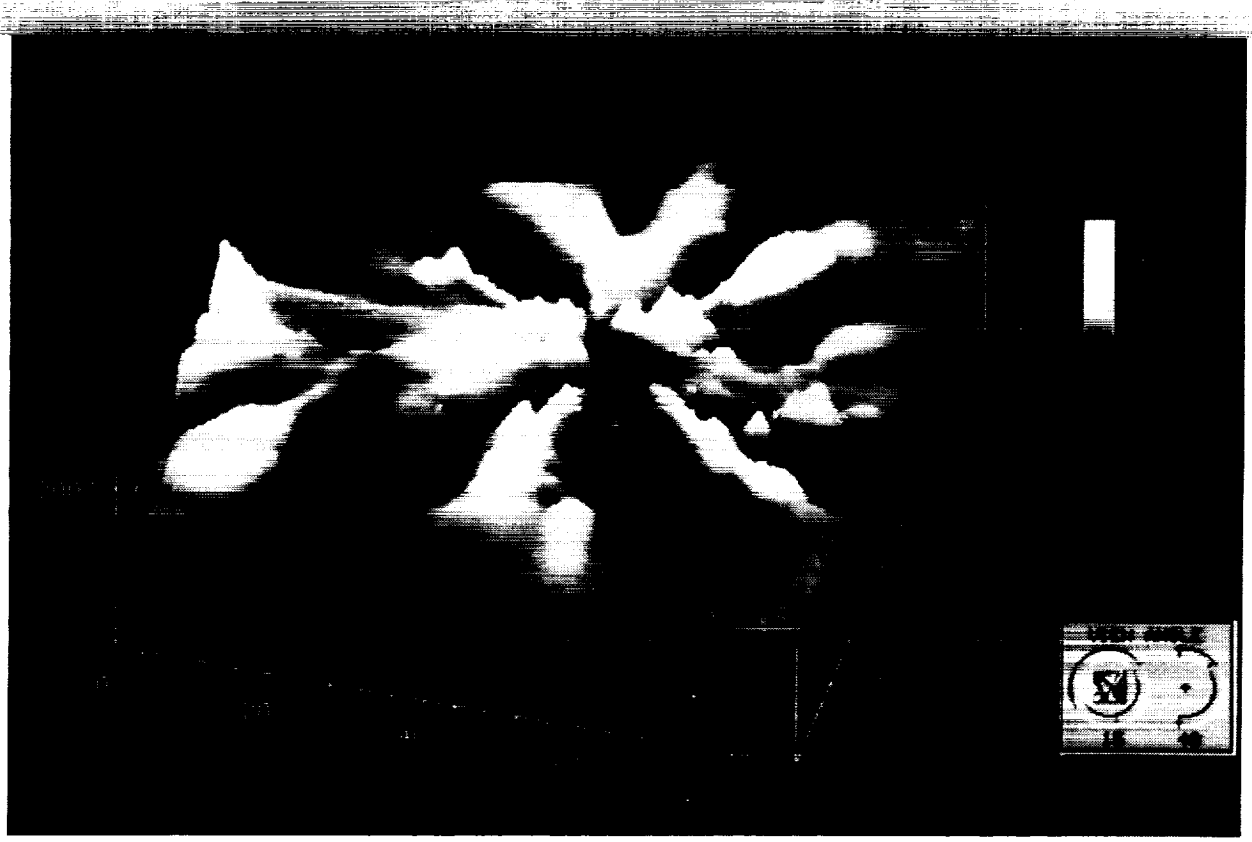

Figure 12b. Atomic force micrograph of secondary impact site in Figure 12a. The melted material around the impact site is an estimated 2000 Å thick.

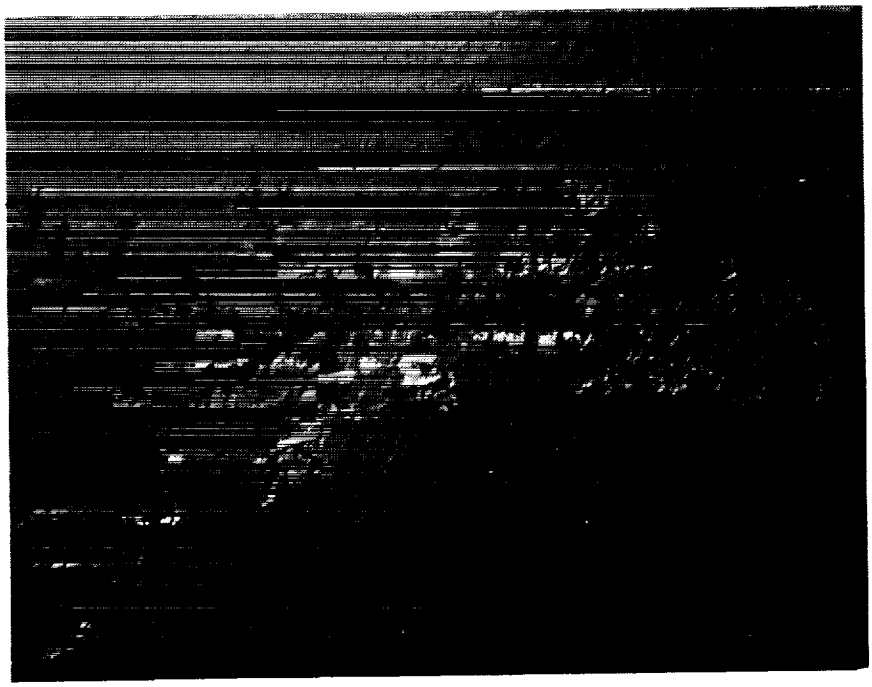

100 μm

Figure 13a. Nomarski micrograph of dendrites on leading-edge $(ZnS/ThF_4)^5Ag/Mo$ test sample, L6-VI-7-68-15. (Note the grain structure of the polished polycrystalline Mo substrate is revealed in the phase-sensitive micrograph.)

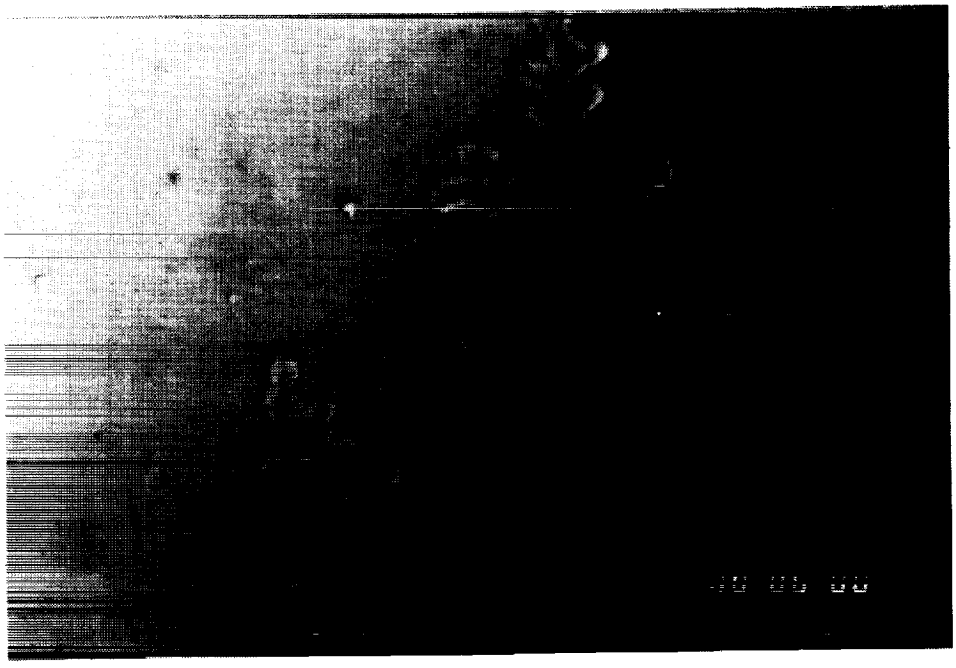

50 μm

Figure 13b. Optical micrograph of dendrites on leading-edge $(ZnS/Al_2O_3)^4Ag/Mo$ test sample, L6-VI-7-67-239. (Micrograph courtesy of S. Gyetvay, Aerospace Corporation.)

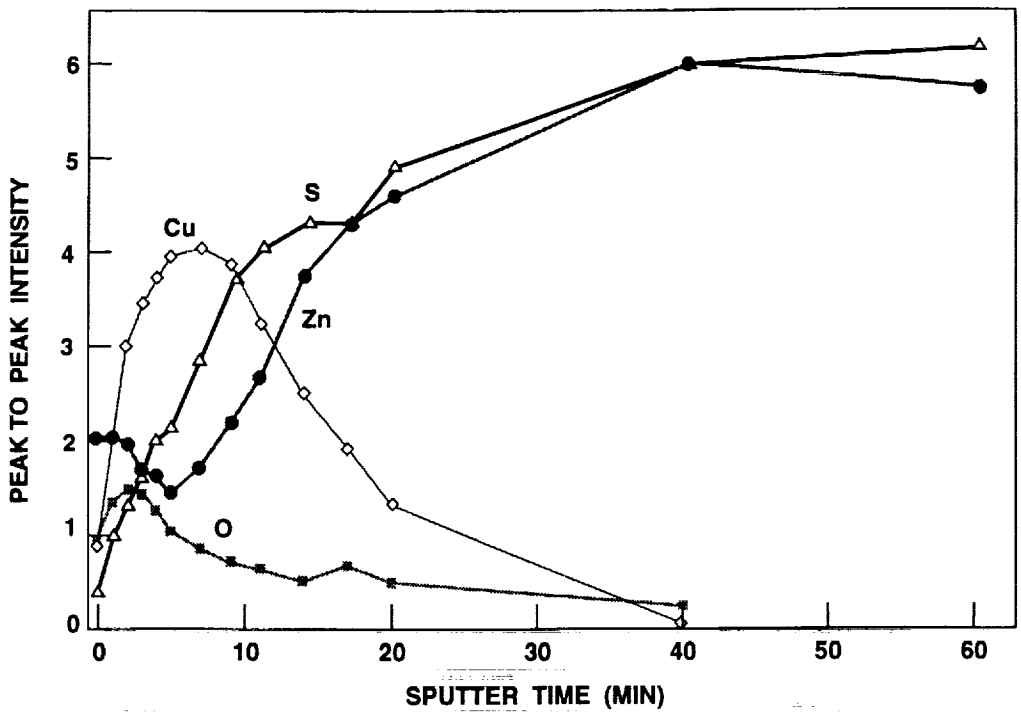

Figure 14. Auger depth profile showing Cu and O reaction with ZnS surface layer in dendrite region of leading-edge test mirror, L6-VI-7-68-15. (Auger depth profile courtesy of T. Beirling and R. Helms, Stanford University.)

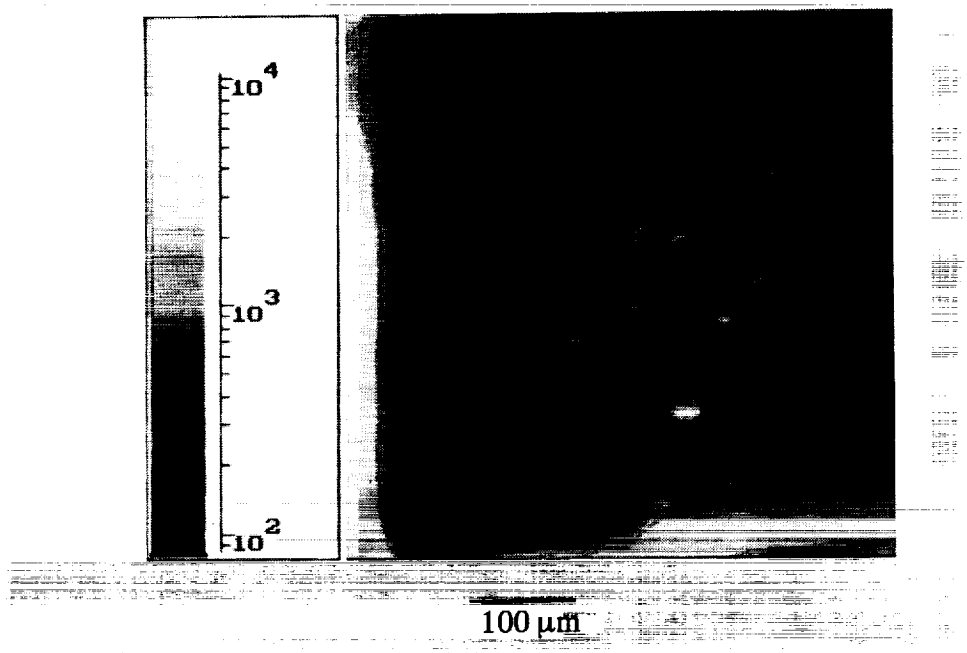

Figure 15. Mass-resolved SIMS image of a dendrite on the leading-edge ZnS-coated test mirror, L6-VI-7-68-15. The bright areas show high concentrations of Al contamination.

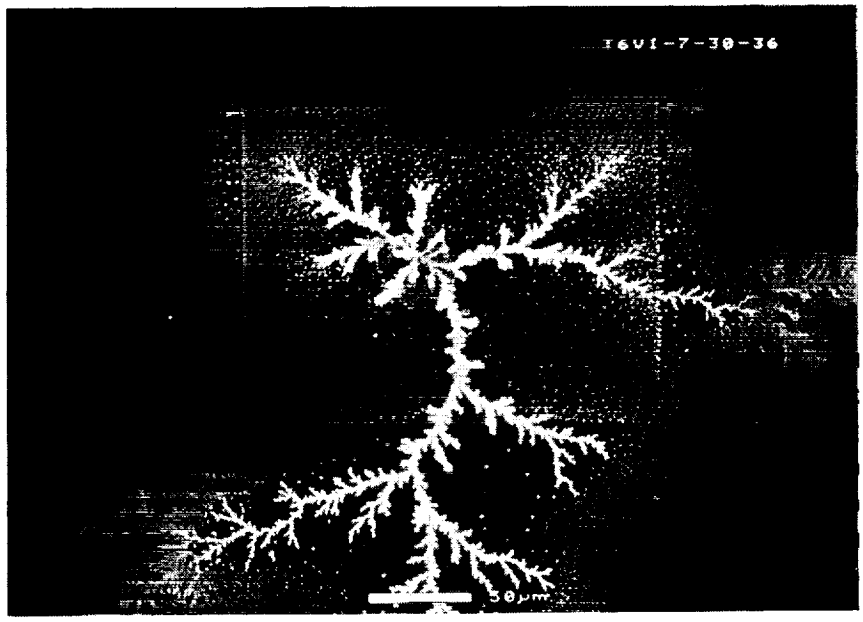

Figure 16. Scanning electron micrograph of dendrite grown in the laboratory on trailing-edge ZnS-coated test mirror, T6-VI-7-30-36. Growth was stimulated by electron irradiation in the region of a secondary impact.

d-5

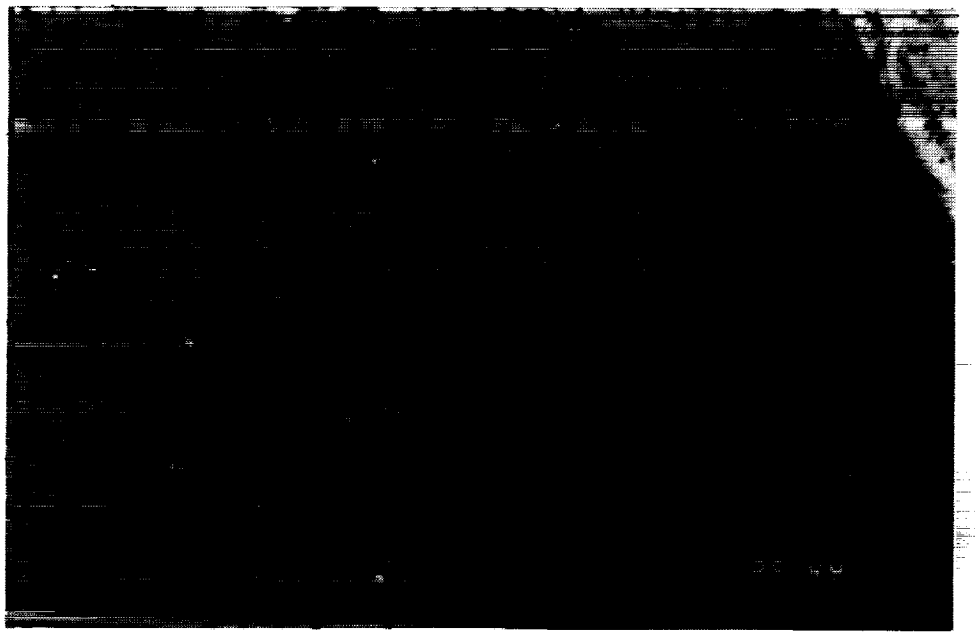

Figure 17a. Optical micrograph of leading-edge ZnS-witness sample (L3-II-7-65-10) after 70-month exposure in LEO. The coating is buckled and annular features are observed at this magnification (168X). (Micrograph courtesy of S. Gyetvay, Aerospace Corporation.)

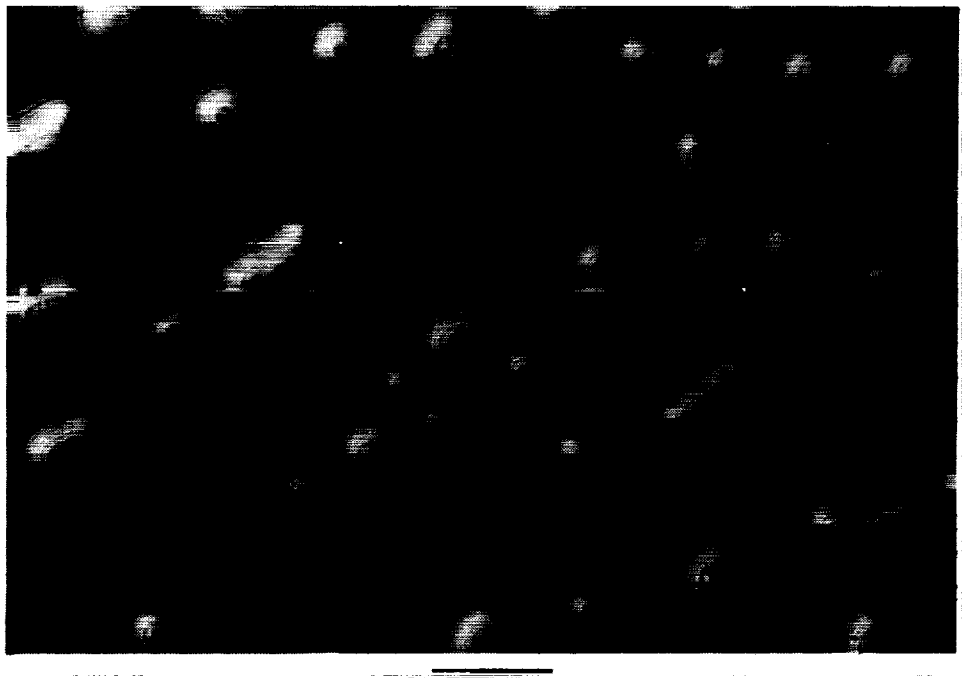

Figure 17b. Optical micrograph of trailing-edge ZnS-witness sample (T3-II-7-64-11) after 70-month exposure in LEO. The coating is mostly intact but many blisters, perhaps related to locally poor adhesion, are observed. (Micrograph courtesy of S. Gyetvay, Aerospace Corporation.)

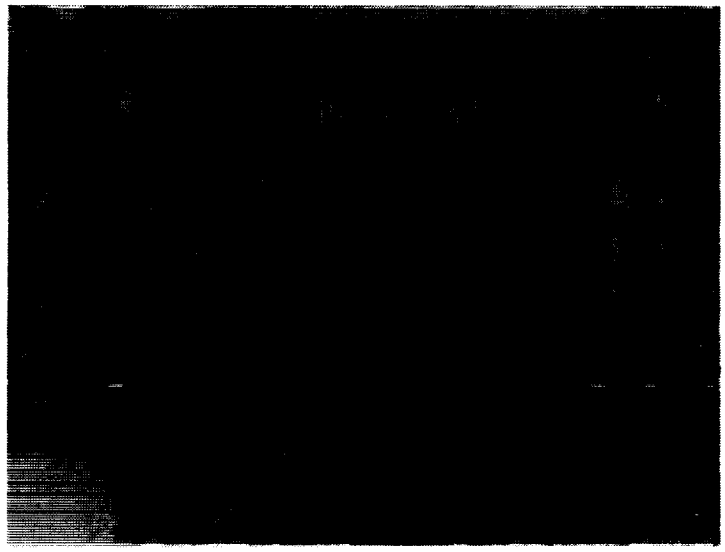

100 μm

Figure 18a. Optical micrograph of a SIMS raster pattern on the leading-edge ZnS-coated test sample, L6-VI-7-68-15. The small crater-like features located within the raster pattern developed as the sample was rastered with a Cs^+ primary ion beam. The source of the crater-like features has not been identified.

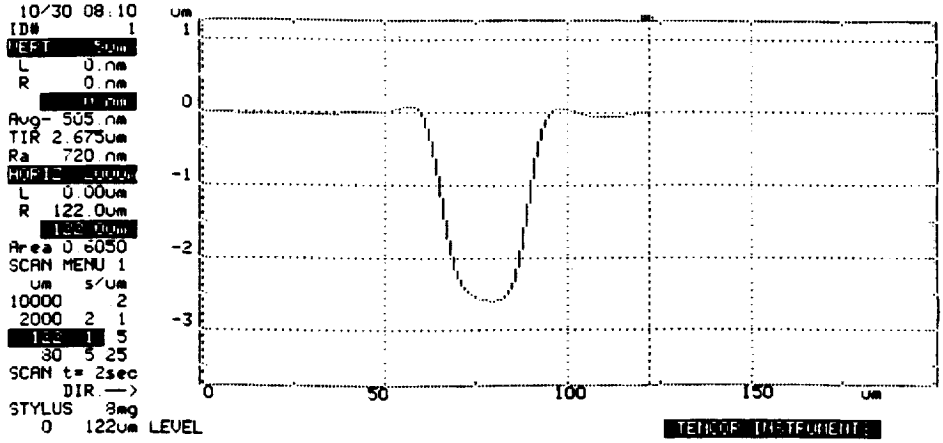

Figure 18b. Profilometer trace through one of the small crater-like features in Figure 18a.